

**Photoswitchable Anticancer Activity via trans-cis
Isomerization of a Combretastatin A-4 Analog**

Journal:	<i>Organic & Biomolecular Chemistry</i>
Manuscript ID	OB-COM-09-2015-002005.R1
Article Type:	Communication
Date Submitted by the Author:	15-Oct-2015
Complete List of Authors:	Sheldon, Jonathan; Virginia Commonwealth University, Chemistry Dcona, Martin; Virginia Commonwealth University, Internal Medicine Lyons, Charles; Virginia Commonwealth University, Massey Cancer Center Hackett, John; Virginia Commonwealth University, Physiology and Biophysics Hartman, Matthew; Virginia Commonwealth University, Chemistry

Photoswitchable Anticancer Activity via *trans-cis* Isomerization of a Combretastatin A-4 Analog

Jonathon E. Sheldon, M. Michael Dcona, Charles E. Lyons, John C. Hackett, and Matthew C. T. Hartman*

Abstract

Combretastatin A-4 (CA4) is highly potent anticancer drug that acts as an inhibitor of tubulin polymerization. The core of the CA4 structure contains a *cis*-stilbene, and it is known that the *trans* isomer is significantly less potent. We prepared an azobenzene analog of CA4 (Azo-CA4) that shows 13-35 fold enhancement in potency upon illumination. EC₅₀ values in the light were in the mid nM range. Due to its ability to thermally revert to less toxic *trans* form, Azo-CA4 also has the ability to automatically turn its activity off with time. Azo-CA4 is less potent than CA-4 because it degrades in the presence of glutathione as evidenced by UV-Vis spectroscopy and ESI-MS. Nevertheless, Azo-CA4 represents a promising strategy for switchable potency for treatment of cancer.

Introduction

Off-target toxicity persists as a challenge in the development and improvement of cancer chemotherapeutics. The use of light is one means to target therapy at the tumor site. In photodynamic therapy (PDT), a photosensitizer is employed to create cytotoxic reactive oxygen species (ROS) at a point of irradiation.^{1,2} One of the clinical challenges involving PDT is that hypoxic tumor microenvironments can limit the ability to create sufficient ROS for therapy.^{3,4} As an alternative, researchers have used light to trigger drug activation or drug delivery. Examples include the release of anti-cancer drugs from a negatively charged, cell-impermeable small molecule along with release from cancer-targeting dendrimers, nanoparticles and liposomes.⁵⁻¹³ Although these methods for targeted drug delivery are promising, in all cases the drug activation is irreversible upon illumination. Very recently, Presa and coworkers have developed Pt(II) complexes with ligands that can be switched

between more toxic and less toxic forms depending on the wavelength of light used.¹⁴ One potential problem for the clinical application of each of these light-activated drug systems is that the activated drug can diffuse away from the illuminated site of the tumor, causing unwanted damage to the tissues it encounters. An ideal light-activated drug would automatically revert to a less potent form over time in order to limit this off-target toxicity. Photoswitchable drugs also offer other unique opportunities in photopharmacology.¹⁵

CA4 (Figure 1) is a tubulin polymerization inhibitor and anticancer drug that exhibits selective cytotoxicity toward tumor vasculature.^{16,17} A variety of cancer cells are highly sensitive to CA4 treatment. EC_{50} values are often under 10 nM.^{18,19} A prodrug of CA4 (CA4-phosphate) is currently being tested in clinical trials in combination with existing chemotherapy agents.^{20,21} In addition, a photocaged version of CA4 has been developed to monitor microtubule dynamics in cells.²² CA4 contains a *cis*-stilbene structure (Figure 1a), which is known to be 60-fold more potent than the *trans* isomer.²³ Light could be used to switch between the two isomers, but this process requires <300 nm UV light which is toxic to cells.²⁴ Azobenzenes contain a molecular backbone that resembles the stilbenoid backbone of CA4, with the olefinic carbon atoms replaced with nitrogens (Figure 1a). Yet, unlike stilbenes, azobenzenes are able to be switched from the *trans* to *cis* form with low intensity light that is compatible with cells.^{25,26} Moreover, when irradiation is terminated, the *cis* form of azobenzenes relaxes back to the thermodynamically stable *trans* form with a half-life that ranges from milliseconds to hours.²⁷⁻²⁹ In principle, therefore, an azobenzene analog of CA4 (Azo-CA4, Figure 1a) will exhibit the dual properties we desired: enhancement in potency with light and automatic turn-off over time.

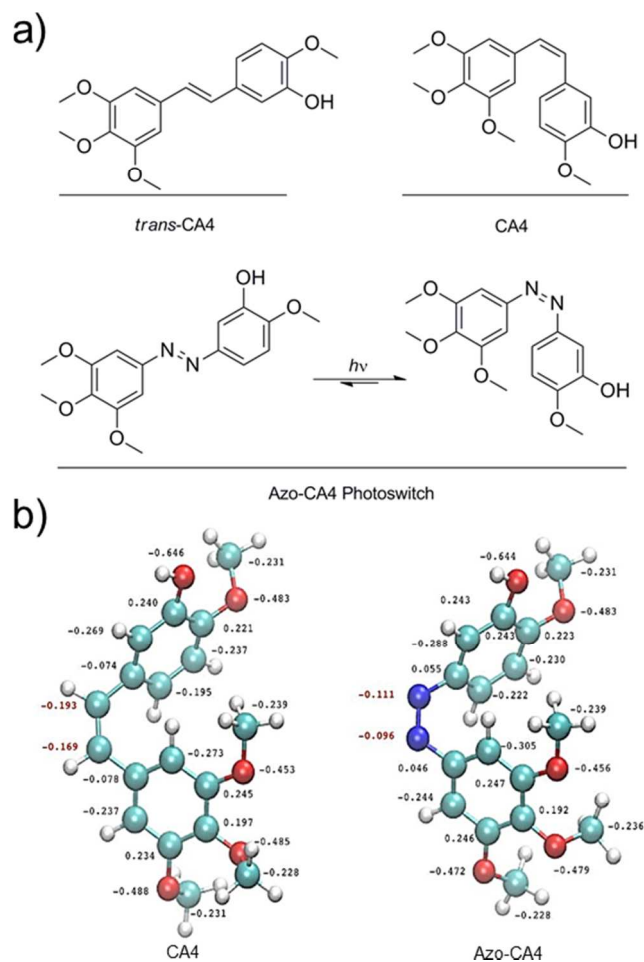


Figure 1. a) Design of Azo-CA4, a photoswitchable analog of CA4. b) RI-MP2/def2-TZVP derived electronic structure of CA4 (left) and Azo-CA4 (right). Labeled charges for non-hydrogen atoms were computed using the natural population analysis method.

Very recently, Borowiak et. al.³⁰ and Engdahl et. al.³¹ reported the synthesis of azobenzene analogs of CA-4 and have extensively investigated their use as tools for controlling tubulin polymerization in cells. They have also reported EC₅₀ values using various light regimes. Herein we add to the knowledge of these exciting compounds, focusing on the effectiveness of their ability to automatically turn off their activity over time, their effects on endothelial cells, and potential limitations for in vivo use.

Experimental

General Methods. All reagents and solvents were purchased from Sigma-Aldrich, VWR, or Fisher Scientific. Reagents for cellular assays were purchased from ATCC, Invitrogen-Gibco, or VWR. The tubulin polymerization assay kit was purchased from Cytoskeleton Inc. ^1H NMR spectra and ^{13}C spectra were recorded at room temperature on a Bruker 400 MHz Ultrashield Plus. Proton and Carbon chemical shifts are expressed in parts per million (ppm, δ scale) and are referenced to the solvent peak. UV-Vis experiments were carried out on either NanoDrop ND-1000 or an Agilent 8453 UV/Vis. Cell Titer Blue (CTB) fluorescence was measured on BioTek Synergy H1 Hybrid plate reader. The UV lamp used in all studies consisted of a simple aquarium light fixture containing two Philips PL-S 9W/2P BLB bulbs. The light was placed at distance of 5 cm from the top of plate. The intensity was measured to be $4.4\text{mW}/\text{cm}^2$.

Compound Synthesis

3-((*tert*-butyldimethylsilyl)oxy)-4-methoxynitrobenzene, 1. To a solution of 2-methoxy-5-nitrophenol (5 g, 29.6 mmol) in DMF (120 mL), TBDMS-Cl (4.90 g, 32.5 mmol) was added in one portion. The reaction mixture was stirred vigorously for 3 hours until TLC showed disappearance of 2-methoxy-5-nitrophenol. The mixture was evaporated and water (80 mL) was added. This solution was extracted 3 times with CH_2Cl_2 (80 mL) and the combined organic layers were washed with brine, dried over Na_2SO_4 , and evaporated to yield 7.73 g (92.3%) of a brown solid. ^1H NMR (400 MHz, CDCl_3) δ 7.89 (dd, $J = 9.0$, 2.8 Hz, 1H), 7.71 (d, $J = 2.7$ Hz, 1H), 6.89 (d, $J = 9.0$ Hz, 1H), 3.92 (s, 3H), 1.01 (s, 9H), 0.19 (s, 6H). ^{13}C NMR (101 MHz, CDCl_3) δ 156.76, 145.01, 141.42, 118.40, 116.06, 110.48, 55.87, 25.60, 18.44, 17.39, -4.63, -4.92. ESI-MS ($\text{M} + \text{H}$) $^+$ $\text{C}_{13}\text{H}_{22}\text{NO}_4\text{Si}^+$ calc 284.1313. obsd 284.1314.

3-((*tert*-butyldimethylsilyl)oxy)-4-methoxyaniline, 2. Compound 1 (2 g, 7.1 mmol) was dissolved in an anhydrous 1:1 mixture of MeOH and EtOH (24 mL) in the presence of 10% Pd/C (400 mg, 0.38 mmol) under Ar. The reaction vessel was purged for 20 minutes with H_2 gas, sealed, and stirred for 3 h. The reaction was filtered through Celite and evaporated to yield 1.69 g (94.5%) of a dark brown oil. ^1H NMR (400 MHz, CDCl_3) δ 6.68 (d, $J = 8.4$ Hz, 1H), 6.28 (d, $J = 2.8$ Hz, 1H), 6.25 (dd, $J = 8.4$, 2.7 Hz, 1H), 3.72 (s, 3H), 3.30 (s, 2H), 0.99 (s, 9H), 0.15 (s, 6H). ^{13}C NMR (101 MHz, CDCl_3) δ 146.12, 144.32, 140.65, 114.43, 109.49, 108.20, 56.62, 25.76, 18.43, -4.36, -4.64. ESI-MS ($\text{M} + \text{H}$) $^+$ $\text{C}_{13}\text{H}_{24}\text{NO}_2\text{Si}^+$ calc 254.1571. obsd 254.1566.

(*E*)-1-(3-((*tert*-butyldimethylsilyl)oxy)-4-methoxyphenyl)-2-(3,4,5-trimethoxyphenyl)diazene, 3. Compound 2 (1 g, 3.9 mmol) and 3,4,5-trimethoxyaniline (723 mg, 3.9 mmol) were stirred in freshly distilled CH_2Cl_2 under Ar. (Diacetoxyiodo)benzene (2.54 g, 7.9 mmol) was added in one portion. The reaction was allowed to proceed until the disappearance of compound 2 via TLC (20 minutes). The reaction mixture was purified by flash column chromatography (100% Hexanes to 20% EtOAc in Hexanes) to yield 107 mg (6.3%) of an orange solid. ^1H NMR (400 MHz, CDCl_3) δ 7.58 (dd, $J = 8.6$, 2.4 Hz, 1H), 7.45 (d, $J = 2.4$ Hz, 1H), 7.21 (s, 2H), 6.96 (d, $J = 8.6$ Hz, 1H), 3.97 (s, 6H), 3.92 (s, 3H), 3.90 (s, 3H), 1.03 (s, 9H), 0.20 (s, 6H). ^{13}C NMR (101 MHz, CDCl_3) δ 153.82, 153.51, 148.69, 146.99, 145.53, 140.16, 119.41, 113.35, 111.20, 100.16, 61.02, 56.22, 55.59, 29.71, 25.74, 18.50, 1.03, -4.56. ESI-MS ($\text{M} + \text{H}$) $^+$ $\text{C}_{22}\text{H}_{33}\text{N}_2\text{O}_5\text{Si}^+$ calc 433.2153. obsd 433.2149.

(E)-2-methoxy-5-((3,4,5-trimethoxyphenyl)diazanyl)phenol, (Azo-CA4) 4. To a solution of compound 3 (53.5 mg, 0.12 mmol) in DMF (4 mL), potassium fluoride hydrate (81.6 mg, 1.4 mmol) and AcOH (20 μ L, 0.35 mmol) were added. The reaction was complete after 1 hour as monitored via TLC. The reaction mixture was evaporated to yield an orange powder. The powder was dissolved in 5 mL CH_2Cl_2 and washed with H_2O (3 x 5 mL), once with brine, and dried over Na_2SO_4 . The organic layer was purified by flash column chromatography (100% Hexanes to 20% EtOAc in Hexanes) to yield 20.6 mg (53.9%) of a waxy orange solid. ^1H NMR (400 MHz, CDCl_3) δ 7.56 – 7.51 (m, 2H), 7.22 (s, 2H), 6.98 (d, J = 8.3 Hz, 1H), 5.72 (s, 1H), 3.98 (s, 3H), 3.96 (s, 6H), 3.93 (s, 3H). ^{13}C NMR (101 MHz, CDCl_3) δ 153.53, 149.20, 148.56, 147.44, 146.23, 140.32, 118.92, 110.09, 106.16, 100.26, 61.02, 56.20. ESI-MS ($M + \text{H}$) $^+$ $\text{C}_{16}\text{H}_{19}\text{N}_2\text{O}_5$ calc 319.1288. obsd 319.1299.

Molar extinction coefficient determination. A 3.1 mM stock solution of Azo-CA4 was prepared in 23% DMSO in water. The solution was stirred vigorously and kept in the dark. 400 μ L of the solution was placed in the each of three tubes and diluted to 1 mL with water to give a final concentration of 1.26 mM Azo-CA4. 2-fold serial dilutions were made and the absorption of each solution was measured on a NanoDrop ND-1000 spectrophotometer. The molar absorptivity, based on three independent trials, was found to be 19,150 $\text{L} \cdot \text{mol}^{-1} \cdot \text{cm}^{-1}$.

Half-Life of thermal relaxation determination. A solution of 300 μ M Azo-CA4 (100 μ L) in either 10% CH_3CN in PBS, 20% CH_3CN , 0.25% DMSO in PBS or 0.25% DMSO in H_2O were placed in a 96 well plate and were irradiated with 380 nm light (4.4 mW/cm^2) for 1 minute. Absorbance readings were taken from triplicate wells every 1 min for 3 h at 37°C and subtracted from the fully relaxed absorbance reading. Data was fitted to a 3-parameter exponential curve (SigmaPlot software).

Azo-CA4 photoswitching integrity assay. A 64 μ M solution of Azo-CA4 in DMSO was placed in a cuvette in an Agilent 8453 UV/VIS at 37°C for 23 hours. The sample was illuminated for 1 min every 3 hours and the absorbance was measured every 5 minutes.

pH sensitivity experiments. A 183 μ M solution of Azo-CA4 in 3.2% DMSO in 50 mM phosphate buffer (pH 8.0) was prepared. The absorption spectrum and pH were measured after multiple additions of small volumes of concentrated HCl.

Glutathione reduction assay. Azo-CA4 (300 μ M in 5.7% DMSO / PBS pH 7.2) in the presence of fully reduced glutathione (10 mM in PBS pH 7.2) and TCEP (5 mM in PBS pH 7.2) was placed in 3 separate wells (100 μ L / well) of a 96 well plate at 37°C. Experiments were performed under UV (380 nm) irradiation (1 min every 2 hours, 4.4 mW/cm^2) or protected from light exposure. For experiments in the light, absorbance readings were collected immediately prior to the subsequent light exposure. Absorbance readings were measured on a BioTek Synergy H1 Hybrid plate reader.

Characterization of glutathione reduction products by ESI-MS. Samples were loaded on a self-packed fused silica (Polymicro Technologies) trap column (360 micron o.d. X 100 micron i.d.) with a Kasil frit packed with 5-15 micron irregular phenyl C-18 YMC packing. The trap column was connected to an analytical column (360 micron o.d. X 50 micron i.d.) with a fritted tip at 5 micron or less (New Objective) packed with 5 μ m phenyl C-18 YMC packing. Peptides were trapped and then eluted into a Thermo Finnigan LCQ deca XP max mass spectrometer with an acetonitrile gradient from 0 % to 80 % over one hour at a flow rate of between 50-150 nl/minute. The mass spectrometer was operated in data dependent mode. First a MS scan from mass 200 or 300-2000 m/z was collected to determine the mass

of molecules eluting at that time, the top two most abundant masses were fragmented into MS/MS scans and placed on an exclusion list. This sequence MS followed by 2 MS/MS scans with exclusion was repeated throughout the 15 minute gradient. Ion chromatograms were plotted of the masses of interest.

***In vitro* Tubulin Polymerization:** Fluorescence *in vitro* tubulin polymerization assays using porcine tubulin were conducted using a fluorescence based polymerization assay kit (Cat. #BK011P; Cytoskeleton, Denver, CO) and following the manufacturers protocol. Each assay was exposed to varying concentrations of Azo-CA4 (80 μ M - 800 nM). Samples were either exposed to light (380 nm, irradiated for 1 minute) or kept in the dark. Irradiated samples of Azo-CA4 were added to tubulin containing wells directly after exposure to light. Azo-CA4 samples kept in the dark were added at the same time and the kinetic assay was started immediately and proceeded for 1 hour at 37°C (Ex. 350nm, Em. 435nm). Samples were normalized to assays lacking Azo-CA4. IC₅₀ values were calculated by fitting the points to the four parameter logistic equation using SigmaPlot software.

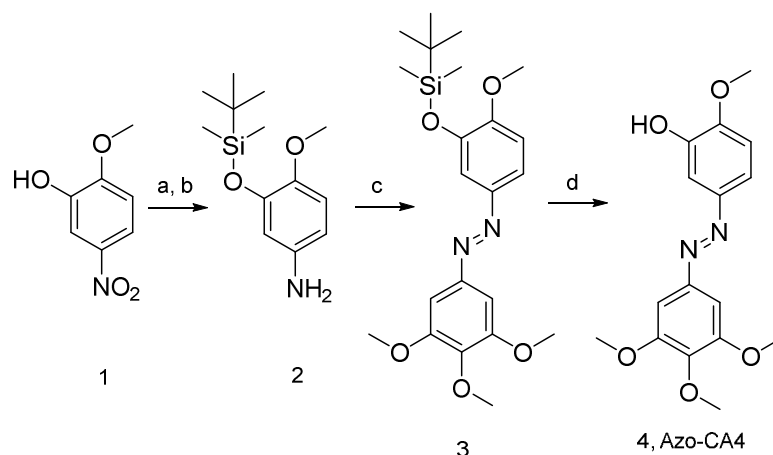
Cell lines and culture conditions. The HUVEC line was cultured in the recommended BASAL media supplemented with VEGF growth factors, 5% Fetal Bovine Serum (FBS, Life Technologies), 2% L-glutamine and 1% of a 10,000 Units/mL Penicillin and 10,000 μ g/mL Streptomycin solution. The MDA-MB-231 line was cultured in DMEM media with supplemented with 10% FBS and 1% of a 10,000 Units/mL Penicillin and 10,000 μ g/mL Streptomycin solution. The T24 line was cultured in McCoy's 5a Medium (ATCC) and supplemented with 10% FBS and 1% of a 10,000 Units/mL Penicillin and 10,000 μ g/mL Streptomycin solution.

Cell viability assays. Cells (18,750 cells/mL for HUVEC, 125,000 cells/mL for MDA-MB-231 and T24 125,000 cells/mL) were seeded in dark, flat bottom 96 well plates with clear lids for > 2 hours in 80 μ L media. After the growing period, Azo-CA4 and CA4 were added at varying concentrations in 20 μ L 0.25% DMSO in media. Various concentrations of Azo-CA4 (30 μ M – 58.6nM for experiments in the light and 100 μ M – 195nM for experiments in the dark) and CA4 (30nM – 0.059nM) were replicated 5 times on each plate. Cells were incubated with drug for 48 hours with one 96 well plate undergoing irradiation at 380nm for 1 minute every hour or every 2 hours for the duration of the experiment and the other kept in the absence of light. 5 wells in each experiment were devoted to media with no cells or cells with vehicle. At the end of the 48 hour time period cells were incubated for 2 hours with 20 μ L Cell Titer Blue reagent (CTB) (Promega) at which time fluorescence was measured on a BioTek Synergy H1 Hybrid plate reader (Ex. 560nm, Em. 590nm). Cell viability was expressed as a percentage of maximum (cells with vehicle) and corrected for background fluorescence of the media. Data is shown as an average \pm S.D. of three independent experiments. GI₅₀ values were calculated using SigmaPlot software using a four parameter logistic equation.

Results

Prior to synthesis of Azo-CA4, we performed a computational study (Figure 1b) to compare its structure to CA4. Both molecules were fully optimized at the RI-MP2/def2-TZVP level of theory and natural population analyses were performed.³² Azo-CA4 was, indeed, highly similar in structure to CA4 (Figure 1b). The optimized geometries and natural charges calculated for non-hydrogen atoms are almost identical with the exception of the nitrogens on the azo bridge. Because the aromatic groups and their methoxy substituents are the major contributors to tubulin binding in CA4,³³ based on structure alone, we would expect that Azo-CA4 would be a potent tubulin inhibitor and act similarly to CA4.

To synthesize Azo-CA4 (Scheme 1), we first protected the phenolic oxygen of nitroaniline **1** with a TBDMS group followed by reduction of the nitro group to give **2**. Compound **2** was coupled to 3,4,5-trimethoxyaniline with diacetoxyiodobenzene³⁴ to yield azobenzene **3** which was separable from homo-aniline coupling side products. Finally, **3** was deprotected with fluoride ion to yield Azo-CA4, **4**.



Scheme 1. Synthesis of Azo-CA4. Reaction conditions: a) TBDMS-Cl, DMF 92%. b) 10% Pd/C, H₂, MeOH/EtOH, 95%. c) 3,4,5-trimethoxyaniline, (diacetoxyiodo)benzene, CH₂Cl₂, 6%. d) KF, AcOH, 95%.

We analyzed the photoswitching properties of Azo-CA4 (Figure 2). The absorbance spectrum of *trans* azo-CA4 showed a λ_{max} of 379 nm and an extinction coefficient consistent with other reports (Figure 2a and SI Figure S1).^{30,35} After 30 seconds of irradiation with 380 nm light, the compound's absorption pattern had dramatically shifted toward an absorption profile that is characteristic for *cis*

azobenzenes^{36,37} (Figure 2a). Over time Azo-CA4 reverted back to the *trans* form with a half-life of 88 min at 37 °C (Figure 2b, 2c and SI Figure S2 and SI Table S1). Multiple cycles of switching and relaxation could be performed over 24 h without degradation (Figure 2d). Surprisingly, the half-life for thermal reversion measured under our conditions was considerably longer than that reported previously.³⁰ To check if the presence of DMSO or buffers caused this change, we measured the photoswitching kinetics under a variety of buffer conditions and light intensities, including those identical to that reported by Borowiak et. al,³⁰ (Figures S2 and S3). Our half-lives for reversion (75-100 min) are consistently much longer than the reported value (6.2 min) even when measured under identical conditions (20% CH₃CN in PBS) (Table S1).

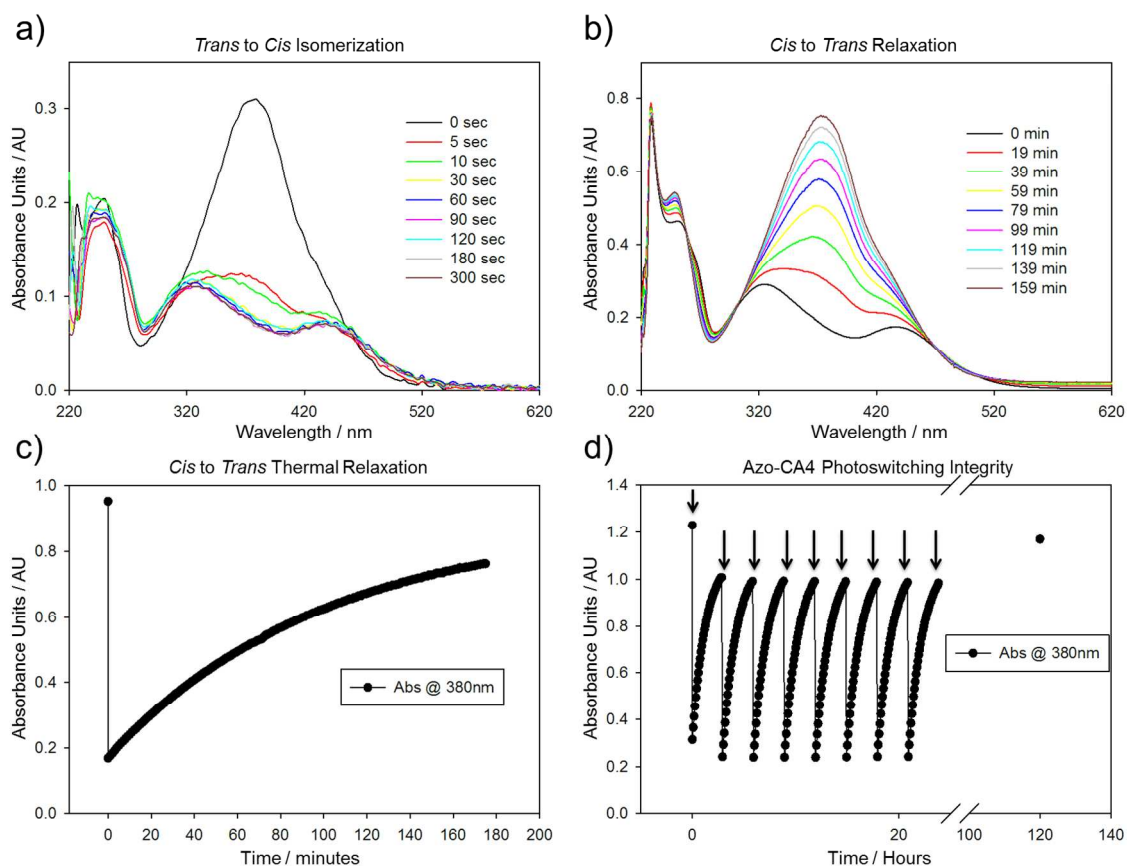


Figure 2. Absorption experiments performed on Azo-CA4. a) Absorption spectra of Azo-CA4 (157 μ M) after exposure to 380 nm light (4.4 mW/cm²) for various amounts of time. b) Absorption spectra demonstrating thermal relaxation over time of Azo-CA4 in the dark at 37°C. Prior to placing in the dark,

Azo-CA4 was treated for 1 minute with 380 nm light ($4.4\text{mW}/\text{cm}^2$). c) Time course of Azo-CA4 relaxation in DMSO monitored by absorbance at 380 nm. d) Time course of 380 nm absorbance of Azo-CA4 over time in DMSO. The sample was irradiated with 380 nm light ($4.4\text{mW}/\text{cm}^2$) for 1 minute every 3 hours at 37°C (arrows). The final point indicates a fully dark-adapted Azo-CA4 left in the dark for 100 hours after the last irradiation.

We then demonstrated that Azo-CA4 inhibits tubulin polymerization in a similar manner to CA4 (SI Figure S4). In vitro experiments were carried out with Azo-CA4 pre-activated with light or in the dark. As expected, in the light Azo-CA4 was a more potent inhibitor of tubulin polymerization than in the dark; light activated Azo-CA4 had an IC_{50} of $5.1\ \mu\text{M}$ (SI Figure S4), similar to the IC_{50} of CA4 ($1.9\ \mu\text{M}$)³⁸ and was 2.8-fold more potent than the dark adapted compound.

Borowiak et. al.³⁰ and Engdahl et. al.³¹ investigated the toxicity of Azo-CA4 on several cancer cell lines. CA4 is a known vasculature-disrupting agent, and we therefore tested the effects of Azo-CA4 on human umbilical vein endothelial cells (HUVECs).^{39,40} For comparison, we also evaluated the effects of Azo-CA4 on a breast adenocarcinoma epithelial cell line (MDA-MB-231) that has shown sensitivity to CA4.⁴¹ Assays with CA4 itself in these cell lines showed EC_{50} s in the low nM range, consistent with other reports (SI Figure S5). With Azo-CA4, we observed significant enhancement of potency in the presence of light vs. untreated controls for both cell lines (Figure 3a and b). Based on the half-lives we determined for *cis* Azo-CA4, we designed several pulse patterns to check for light-enabled toxicity ranging from a single 1 minute pulse at the beginning of the experiment, to a 1 minute pulse every 60 minutes (Figure 3c). As expected with the turn-off mechanism, we saw decreasing EC_{50} values as the duration between pulses decreased (Table 1). For the 1 h pulse regime, Azo-CA4 was 22-fold more toxic to HUVEC cells than dark controls. Light alone at the same doses was not toxic for either cell line (Figure 3d).

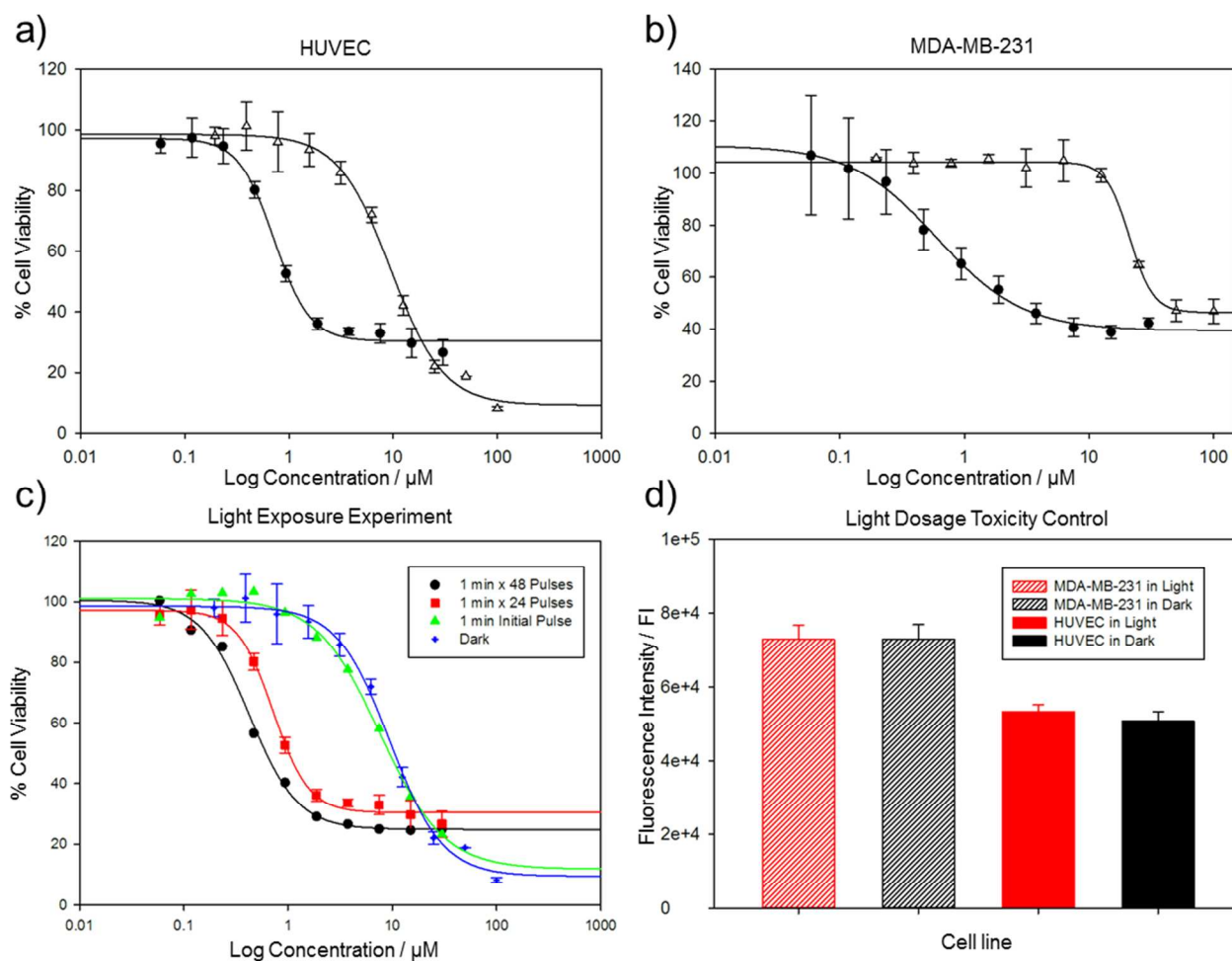


Figure 3. Analysis of the inhibition of Azo-CA4 in cell culture. Cells were treated with varying concentrations of Azo-CA4 for 48 hours and were either exposed to 380 nm light (4.4 mW/cm^2) (closed circles) or kept in the dark (open triangles). In (a) HUVEC cells were treated with light for 1 min every 2 h. In (b) MDA-MD-231 cells were treated with light for 1 min every 1 h. In (c) HUVEC cells were treated 1 minute light pulses at varying intervals: No light (Black circles), 1x1 minute at the beginning of the experiment (Green triangles), 24x1 minute (every 2 h), and 48x1 minute (every 1 h). Cell viability assays reported as a percentage of vehicle controls. The value in parentheses is the EC_{50} . In (d), the cells were treated with 380 nm light (4.4 mW/cm^2 , 1 minute every hour) or kept in the dark for 48 h followed by analysis of cell density with Cell Titer Blue.

Table 1. EC₅₀ values of cell viability assays with Azo-CA4 and CA4. Results of varying light dosages in HUVEC cells are shown.

	MDA-MB-231 ^[a]	HUVEC ^[b]	HUVEC ^[c]	HUVEC ^[d]
Azo-CA4 Light	0.6 ± 0.07 μM	0.4 ± 0.03 μM	0.7 ± 0.04 μM	7.7 ± 1.5 μM
Azo-CA4 Dark	21.1 ± 0.6 μM	9.5 ± 0.8 μM	-	-
CA4	0.0037 ± 0.2 μM	0.0021 ± 0.2 μM	-	-

[a] Cell viability assay with light pulse for 1 min every 1 hour. Error represents triplicate experiments. [b] Cell viability assay with light pulse for 1 min every 1 hour. Error represents 5 wells. [c] Cell viability assay with light pulse for 1 min every 2 hours. Error represents triplicate experiments. [d] Cell viability assay with light pulse for 1 min at beginning of experiment. Error represents 5 wells.

The significant gap between the cytotoxicity of CA4 and Azo-CA4 in these cell lines suggested that Azo-CA4 may be unstable in cells. Since azobenzenes are known to react with glutathione (GSH),^{42,43} we evaluated the extent to which GSH could inactivate Azo-CA4 (Figure 4 and SI Figure S6). Both forms of Azo-CA4 were degraded by GSH over the course of several hours. Interestingly, the light-activated *cis*-Azo-CA4 compounds were degraded more rapidly than *trans*-Azo-CA4, and this effect could limit the potency at higher light doses when more *cis*-Azo-CA4 is present.

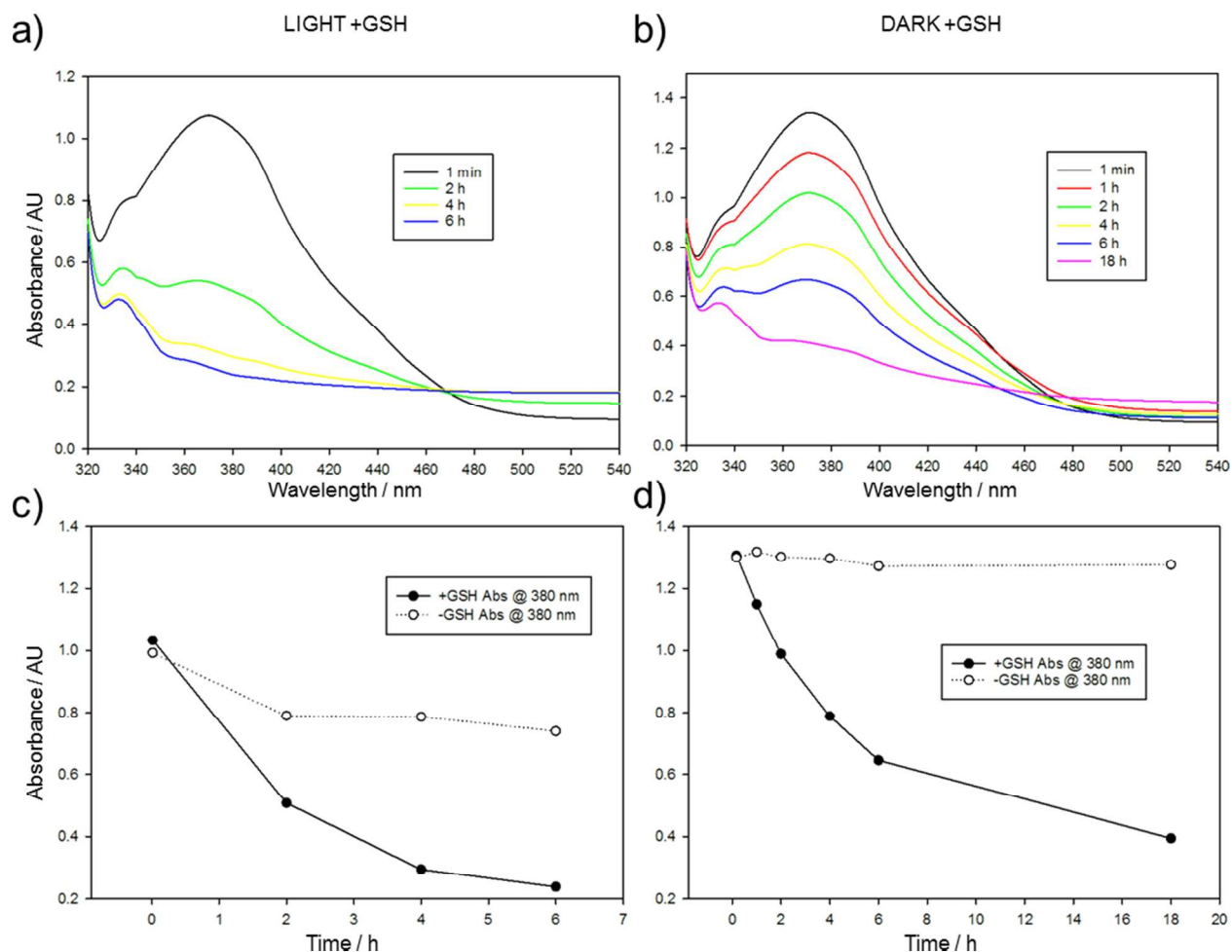


Figure 4. Glutathione exposure in light. Azo-CA4 (300 μM in 5.7% DMSO / PBS pH 7.2) in the presence of fully reduced glutathione (10 mM in PBS pH 7.2) and TCEP (5 mM in PBS pH 7.2) was placed in 3 separate wells (100 μL / well) of a 96 well plate at 37°C and (a) exposed to light (380 nm, 4.4 mW/cm^2) for 1 min every 2 h. Absorbance spectra were taken at different time points directly preceding exposure to light and are expressed as an average of triplicate readings. (b) is identical to (a) except the reaction was kept in the dark, and the Azo-CA4 concentration was 400 μM . (c) and (d) plot the change absorbance of 380 nm over time of the data in (a) and (b) compared to identical reactions lacking glutathione. The decrease in absorbance of the minus GSH control in (c) is due to incomplete relaxation back to the *trans* state.

To investigate this further, we treated our compound with light and GSH and followed the course of the reaction by LC-MS/MS (Figure 5 and SI Figures S7-S9). As expected, the peak corresponding to the *cis*-Azo-CA4 decreased over time (Figure 5a and SI Figure S7). Surprisingly, a new peak of the same mass was formed during the reaction. This peak did not co-elute with *trans*-Azo-CA4 (SI Figure S8), and therefore must be due to a rearrangement product or products. (Note also that the samples were irradiated with light immediately prior to injection which would have eliminated the majority of the *trans* isomer even if was present beforehand). Additionally, transient formation of a peak of 624 Da was observed during the reaction. The MS-MS fragmentation of this peak showed neutral loss peaks of 307, 275, and 129, all of which are characteristic for GSH adducts (SI Figure S7).⁴⁴ This peak was not present in a control reaction lacking Azo-CA4 (SI figure S9), lending credence to the fact that this species is an adduct of glutathione and Azo-CA4.

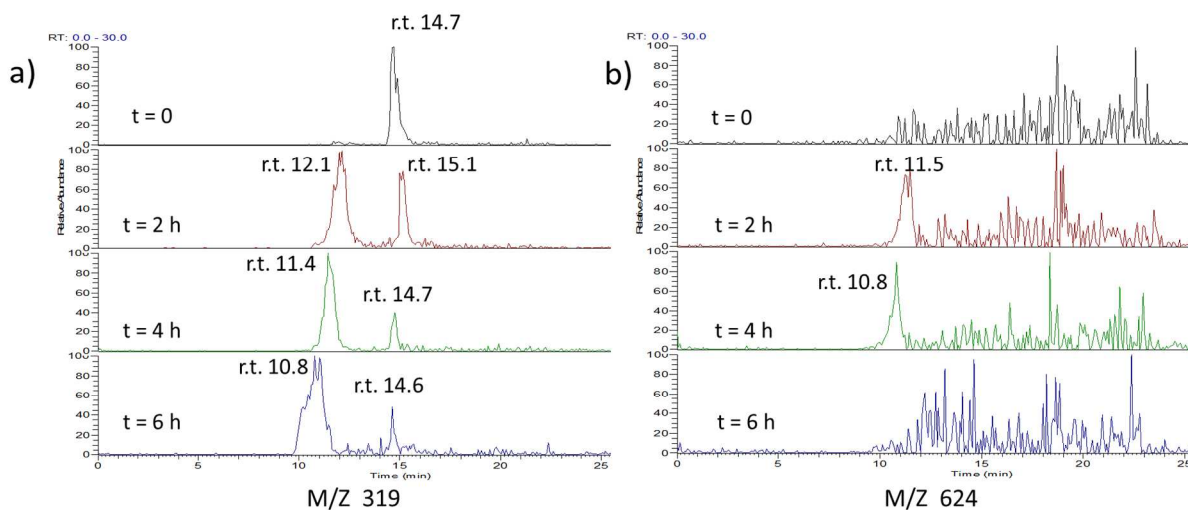


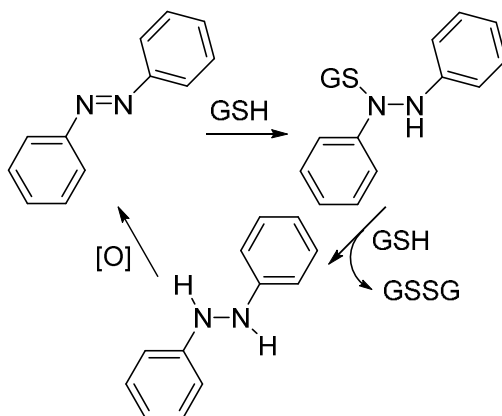
Figure 5. ESI-MS analysis of the reaction of glutathione and Azo-CA4. Azo-CA4 (300 μM in 5.7% DMSO / PBS pH 7.2) in the presence of fully reduced glutathione (10 mM in PBS pH 7.2) and TCEP (5 mM in PBS pH 7.2) was placed in 3 separate wells (100 μL / well) of a 96 well plate at 37°C and exposed to light (380 nm, 4.4 mW/cm^2) for 1 min every 2 h immediately preceding analysis. At the times given, a sample was removed and injected onto an analytical column containing 5 μm phenyl C-18 YMC and analyzed by ESI-MS. (a) Traces for ions of M+H identical to Azo-CA4 (319 Da). (b) Traces corresponding to M/Z of 624 Da. Slight retention time drifts are expected due to manual loading of the capillary containing sample onto the instrument (see Figure S7 for the LC-MS spectra of co-injected standards).

Discussion

The half-life of thermal reversion of Azo-CA4 and its future analogs is a critical piece of their potential use as automatic turn-off drugs and tools.¹⁵ It is therefore significant that our values for the half-lives of Azo-CA4 vary significantly from those determined by Borowiak et. al. under the same conditions; our value is about 14-fold longer (85 min vs. 6.2 min).³⁰ Although in cells the half-life of Azo-CA4 can be altered by thiols, the cellular environment,¹⁵ and by tubulin binding itself, all of our cell culture data supports the longer half-life value. For example, our measured EC₅₀ values for Azo-CA4 with MDA-231 cells are very similar to those determined by Borowiak et al on this cell line,³⁰ yet we pulsed with light once per hour, and they pulsed every 15 seconds. If the half-life was 6.2 minutes as reported,³⁰ we should have observed significantly weaker potency with our pulse regimen.

Glutathione reactions with azobenzenes have been studied on a number of systems. For most azobenzenes, nucleophilic attack of GS⁻ anion on the diazo nitrogen gives the intermediate sulfenylhydrazide⁴⁵ (Scheme 2). The sulfenyl hydrazide is then either attacked by a second glutathione anion to displace the reduced hydrazide or is hydrolyzed by water to give back the azobenzene plus a sulfenic acid (Scheme 2). The hydrazide is easily oxidized back to the azobenzene, and therefore, the net result of each of these reactions is re-formation of the original *trans*-azobenzene. By a similar mechanism, glutathione catalyzes the relaxation of *cis*-azobenzenes back into their *trans* form.^{15,46} With Azo-CA4; however, our data shows that reaction with glutathione leads to the destruction of the azobenzene structure. This has been observed before by Woolley with other electron rich methoxy-substituted azobenzenes.^{41,42,47} Woolley proposed that the enhanced basicity of the electron rich azo nitrogens leads to protonation which primes the compound for nucleophilic attack by GSH. However, this proposed mechanism leads to the production of the same sulfenyl hydrazide (Scheme 2) that would be expected to result in reversion back to the azobenzene. We measured the pKa of Azo-CA4, and it is below 4.6 (SI Figure S10), so it will not be protonated at physiological pH. Moreover, we did not see any

ions corresponding either to the mass of the phenylhydrazide or the sulfenylhydrazide during the course of the reaction. Instead, our LC-MS data shows that a transient adduct of Azo-CA4 and GSH with a mass of 624 is formed during the GSH reaction. This mass is two less than would be expected for the sulfenyl hydrazide. The formation of this 624 Da species could potentially be explained by nucleophilic attack of the azo nitrogen onto GSSG to form the sulfenyl diazo cation. To test this, we incubated Azo-CA4 with GSSG, but no reaction was observed over 18 h (data not shown) which rules out this potential mechanism. One could envision other possibilities for formation of the sulfenyl diazo cation, or loss of the two hydrogens via a mechanism involving electrocyclicization of the two rings. Since the light-activated Azo-CA4 degrades more rapidly than that in the dark (Figure 4c), photochemical pathways for degradation that also involve GSH could also be envisioned. More work needs to be done to distinguish between these and other possibilities. Importantly, to our knowledge, this type of degradation has only been observed with electron-rich azobenzenes, which suggests that addition of electron withdrawing substituents could eliminate or slow the degradation pathway.



Scheme 2. Reactions of azobenzenes with glutathione. Reported reaction cycle of azobenzenes with glutathione.

In summary, Azo-CA4 exhibits remarkable enhancements in potency against HUVEC cells that are consistent with its ability to switch into the more toxic *cis* form in the presence of light. Moreover, over time, Azo-CA4 automatically converts back to its less toxic form. Provided the glutathione

reactivity issue can be solved, Azo-CA4 and future, similar compounds offer the potential for automatic turn-off of drug activity in sites distal from the site of activation and thus present a novel means for tightly controlling drug potency and antitumor activity.

References

1. Dolmans, D. E.; Fukumura, D.; Jain, R. K. Photodynamic therapy for cancer. *Nat. Rev. Canc* **2003**, *3*, 380-387.
2. Robertson, C.; Evans, D. H.; Abrahamse, H. Photodynamic therapy (PDT): a short review on cellular mechanisms and cancer research applications for PDT. *J. Photochem. Photobiol. B* **2009**, *96*, 1-8.
3. Henderson, B. W.; Dougherty, T. J. How Does Photodynamic Therapy work? *Photochem. Photobiol.* **1992**, *55*, 145-157.
4. Brian C Wilson and Michael, S. Patterson The physics, biophysics and technology of photodynamic therapy. *Phys. Med. Biol.* **2008**, *53*, R61.
5. Michael Dcona, M.; Yu, Q.; Capobianco, J. A.; Hartman, M. C. T. Near infrared light mediated release of doxorubicin using upconversion nanoparticles. *Chem. Commun.* **2015**, *51*, 8477-8479.
6. Dcona, M. M.; Mitra, D.; Goehe, R. W.; Gewirtz, D. A.; Lebman, D. A.; Hartman, M. C. T. Photocaged permeability: a new strategy for controlled drug release. *Chem. Commun.* **2012**, *48*, 4755-4757.
7. Ki Choi, S.; Thomas, T.; Li, M.; Kotlyar, A.; Desai, A.; Baker, J., James R. Light-controlled release of caged doxorubicin from folate receptor-targeting PAMAM dendrimer nanoconjugate. *Chem. Commun.* **2010**, *46*, 2632-2634.
8. You, J.; Zhang, G.; Li, C. Exceptionally High Payload of Doxorubicin in Hollow Gold Nanospheres for Near-Infrared Light-Triggered Drug Release. *ACS Nano* **2010**, *4*, 1033-1041.
9. You, J.; Zhang, P.; Hu, F.; Du, Y.; Yuan, H.; Zhu, J.; Wang, Z.; Zhou, J.; Li, C. Near-Infrared Light-Sensitive Liposomes for the Enhanced Photothermal Tumor Treatment by the Combination with Chemo.. *Pharm. Res.* **2014**, *31*, 554-565.
10. Agasti, S. S.; Chompoosor, A.; You, C.; Ghosh, P.; Kim, C. K.; Rotello, V. M. Photoregulated Release of Caged Anticancer Drugs from Gold Nanoparticles. *J. Am. Chem. Soc.* **2009**, *131*, 5728-5729.
11. Fedoryshin, L. L.; Tavares, A. J.; Petryayeva, E.; Doughan, S.; Krull, U. J. Near-Infrared-Triggered Anticancer Drug Release from Upconverting Nanoparticles. *ACS Appl. Mater. Inter.* **2014**, *6*, 13600-13606.
12. Hu, X.; Tian, J.; Liu, T.; Zhang, G.; Liu, S. Photo-Triggered Release of Caged Camptothecin Prodrugs from Dually Responsive Shell Cross-Linked Micelles. *Macromolecules* **2013**, *46*, 6243-6256.

13. Xing, Q.; Li, N.; Jiao, Y.; Chen, D.; Xu, J.; Xu, Q.; Lu, J. Near-infrared light-controlled drug release and cancer therapy with polymer-caged upconversion nanoparticles. *RSC Adv.* **2015**, *5*, 5269-5276.
14. Presa, A.; Brissos, R. F.; Caballero, A. B.; Borilovic, I.; Korrodi-Gregório, L.; Pérez-Tomás, R.; Roubeau, O.; Gamez, P. Photoswitching the Cytotoxic Properties of Platinum(II) Compounds. *Angew. Chem. Int. Ed.* **2015**, *54*, 4561-4565.
15. Velema, W. A.; Szymanski, W.; Feringa, B. L. Photopharmacology: beyond proof of principle. *J. Am. Chem. Soc.* **2014**, *136*, 2178-2191.
16. Pettit, G. R.; Singh, S. B.; Boyd, M. R.; Hamel, E.; Pettit, R. K.; Schmidt, J. M.; Hogan, F. Antineoplastic agents. 291. Isolation and synthesis of combretastatins A-4, A-5, and A-6(1a). *J. Med. Chem.* **1995**, *10*, 1666-1672.
17. Pettit, G. R.; Cragg, G. M.; Herald, D. L.; Schmidt, J. M.; Lohavanijaya, P. Isolation and structure of combretastatin. *Can. J. Chem.* **1982**, *60*, 1374-1376.
18. Sharma, V. M.; Adi Seshu, K. V.; Vamsee Krishna, C.; Prasanna, P.; Chandra Sekhar, V.; Venkateswarlu, A.; Rajagopal, S.; Ajaykumar, R.; Deevi, D. S.; Rao Mamidi, N. V. S.; Rajagopalan, R. Novel 6,7-diphenyl-2,3,8,8a-tetrahydro-1H-indolizin-5-one analogues as cytotoxic agents. *Bioorg. Med. Chem. Lett.* **2003**, *13*, 1679-1682.
19. Dorr, R.; Dvorakova, K.; Snead, K.; Alberts, D.; Salmon, S.; Pettit, G. R. Antitumor activity of combretastatin-A4 phosphate, a natural product tubulin inhibitor. *Invest. New Drugs.* **1996**, *14*, 131-137.
20. Nathan, P.; Zweifel, M.; Padhani, A. R.; Koh, D.; Ng, M.; Collins, D. J.; Harris, A.; Carden, C.; Smythe, J.; Fisher, N.; Taylor, N. J.; Stirling, J. J.; Lu, S.; Leach, M. O.; Rustin, G. J. S.; Judson, I. Phase I Trial of Combretastatin A4 Phosphate (CA4P) in Combination with Bevacizumab in Patients with Advanced
21. Rustin, G. J. S.; Galbraith, S. M.; Anderson, H.; Stratford, M.; Folkes, L. K.; Sena, L.; Gumbrell, L.; Price, P. M. Phase I Clinical Trial of Weekly Combretastatin A4 Phosphate: Clinical and Pharmacokinetic Results. *J. Clin. Onc.* **2003**, *21*, 2815-2822.
22. Wühr, M.; Tan, E. S.; Parker, S. K.; Detrich, H. W.; Mitchison, T. J. A model for cleavage plane determination in early amphibian and fish embryos. *Current Biology* **2010**, *20*, 2040-2045.
23. Lawrence, N. J.; Rennison, D.; Woo, M.; McGown, A. T.; Hadfield, J. A. Antimitotic and cell growth inhibitory properties of combretastatin A-4-like ethers. *Bioorg. Med. Chem. Lett.* **2001**, *11*, 51-54.
24. Figueiras, T.; Neves-Petersen, M.; Petersen, S. Activation Energy of Light Induced Isomerization of Resveratrol. *J. Fluoresc.* **2011**, *21*, 1897-1906.
25. Beharry, A. A.; Woolley, G. A. Azobenzene photoswitches for biomolecules. *Chem. Soc. Rev.* **2011**, *40*, 4422-4437.

26. Lednev, I. K.; Ye, T. -.; Matousek, P.; Towrie, M.; Foggi, P.; Neuwahl, F. V. R.; Umopathy, S.; Hester, R. E.; Moore, J. N. Femtosecond time-resolved UV-visible absorption spectroscopy of trans-azobenzene: dependence on excitation wavelength. *Chem. Phys. Lett.* **1998**, *290*, 68-74.
27. Broichhagen, J.; Sch||nberger, M.; Cork, S. C.; Frank, J. A.; Marchetti, P.; Bugliani, M.; Shapiro, A. M. J.; Trapp, S.; Rutter, G. A.; Hodson, D. J.; Trauner, D. Optical control of insulin release using a photoswitchable sulfonyleurea. *Nat. Commun.* **2014**, *5*.
28. Pittolo, S.; G||mez-Santacana, X.; Eckelt, K.; Rovira, X.; Dalton, J.; Goudet, C.; Pin, J.; Llobet, A.; Giraldo, J.; Llebaria, A.; Gorostiza, P. An allosteric modulator to control endogenous G protein-coupled receptors with light. *Nat. Chem. Biol.* **2014**, *10*, 813-815.
29. Kumita, J. R.; Smart, O. S.; Woolley, G. A. Photo-Control of Helix Content in a Short Peptide. *Proc. Natl. Acad. Sci. U. S. A.* **2000**, *97*, 3803-3808.
30. Borowiak, M.; Nahaboo, W.; Reynders, M.; Nekolla, K.; Jalinot, P.; Hasserodt, J.; Rehberg, M.; Delattre, M.; Zahler, S.; Vollmar, A.; Trauner, D.; Thorn-Seshold, O. Photoswitchable Inhibitors of Microtubule Dynamics Optically Control Mitosis and Cell Death. *Cell.* **162**, 403-411.
31. Engdahl, A. J.; Torres, E. A.; Lock, S. E.; Engdahl, T. B.; Mertz, P. S.; Streu, C. N. Synthesis, Characterization, and Bioactivity of the Photoisomerizable Tubulin Polymerization Inhibitor azo-Combretastatin A4. *Org. Lett.* **2015**, *17*, 4546-4549.
32. Reed, A. E.; Weinstock, R. B.; Weinhold, F. Natural population analysis. *J. Chem. Phys.* **1985**, *83*, 735-746.
33. Jin, Y.; Qi, P.; Wang, Z.; Shen, Q.; Wang, J.; Zhang, W.; Song, H. 3D-QSAR Study of Combretastatin A-4 Analogs Based on Molecular Docking. *Molecules.* **2011**, *16*, 6684-6700.
34. Monir, K.; Ghosh, M.; Mishra, S.; Majee, A.; Hajra, A. Phenyl iodine(III) Diacetate (PIDA) Mediated Synthesis of Aromatic Azo Compounds through Oxidative Dehydrogenative Coupling of Anilines: Scope and Mechanism. *Eur. J. of Org. Chem.* **2014**, *2014*, 1096-1102.
35. Bandara, H. M. D.; Burdette, S. C. Photoisomerization in different classes of azobenzene. *Chem. Soc. Rev.* **2012**, *41*, 1809-1825.
36. Birnbaum, P. P.; Linford, J. H.; Style, D. W. G. The absorption spectra of azobenzene and some derivatives. *Trans. Faraday Soc.* **1953**, *49*, 735-744.
37. Liu, D.; Karanicolas, J.; Yu, C.; Zhang, Z.; Woolley, G. A. Site-specific incorporation of photoisomerizable azobenzene groups into ribonuclease S. *Bioorg. Med. Chem. Lett.* **1997**, *7*, 2677-2680.
38. Cushman, M.; Nagarathnam, D.; Gopal, D.; Chakraborti, A. K.; Lin, C. M.; Hamel, E. Synthesis and evaluation of stilbene and dihydrostilbene derivatives as potential anticancer agents that inhibit tubulin polymerization. *J. Med. Chem.* **1991**, *34*, 2579-2588.

39. Vincent, L.; Kermani, P.; Young, L. M.; Cheng, J.; Zhang, F.; Shido, K.; Lam, G.; Bompais-Vincent, H.; Zhu, Z.; Hicklin, D. J.; Bohlen, P.; Chaplin, D. J.; May, C.; Rafii, S. Combretastatin A4 phosphate induces rapid regression of tumor neovessels and growth through interference with vascular endothelial-cadherin signaling. *J. Clin. Invest.* **2005**, *115*, 2992-3006.
40. Dark, G. G.; Hill, S. A.; Prise, V. E.; Tozer, G. M.; Pettit, G. R.; Chaplin, D. J. Combretastatin A-4, an Agent That Displays Potent and Selective Toxicity toward Tumor Vasculature. *Canc. Res.* **1997**, *57*, 1829-1834.
41. Parihar, S.; Kumar, A.; Chaturvedi, A. K.; Sachan, N. K.; Luqman, S.; Changkija, B.; Manohar, M.; Prakash, O.; Chanda, D.; Khan, F.; Chanotiya, C. S.; Shanker, K.; Dwivedi, A.; Konwar, R.; Negi, A. S. Synthesis of combretastatin A4 analogues on steroidal framework and their anti-breast cancer activity. *J. Steroid Biochem. Mol. Biol.* **2013**, *137*, 332-344.
42. Samanta, S.; Beharry, A. A.; Sadovski, O.; McCormick, T. M.; Babalhavaeji, A.; Tropepe, V.; Woolley, G. A. Photoswitching Azo Compounds in Vivo with Red Light. *J. Am. Chem. Soc.* **2013**, *135*, 9777-9784.
43. Samanta, S.; McCormick, T. M.; Schmidt, S. K.; Seferos, D. S.; Woolley, G. A. Robust visible light photoswitching with ortho-thiol substituted azobenzenes. *Chem. Commun.* **2013**, *49*, 10314-10316.
44. Murphy, C. M.; Fenselau, C.; Gutierrez, P. L. Fragmentation characteristic of glutathione conjugates activated by high-energy collisions. *J. Am. Soc. Mass Spectrom.* **1992**, *3*, 815-822.
45. Boulègue, C.; Löweneck, M.; Renner, C.; Moroder, L. Redox potential of azobenzene as an amino acid residue in peptides. *ChemBioChem* **2007**, *8*, 591-594.
46. Standaert, R. F.; Park, S. B. Abc amino acids: design, synthesis, and properties of new photoelastic amino acids. *J. Org. Chem.* **2006**, *71*, 7952-7966.
47. Samanta, S.; McCormick, T. M.; Schmidt, S. K.; Seferos, D. S.; Woolley, G. A. Robust visible light photoswitching with ortho-thiol substituted azobenzenes. *Chem. Commun.* **2013**, *49*, 10314-10316.